

The Role of C–H···O Interactions in the Solid and Liquid-Phase Structures of Methyltrioxo Rhenium

Pedro D. Vaz,^{*,[a,b]} and Paulo J. A. Ribeiro-Claro^[a]

Keywords: Rhenium / C–H···O Hydrogen bonds / Ab initio calculations / Raman spectroscopy / Inelastic neutron scattering

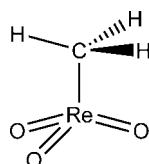
The importance of C–H···O hydrogen bonds involving the less common Re=O acceptor group in the small organometallic methyltrioxorhenium (MTO) is studied by combined vibrational spectroscopy and ab initio calculations. The observed vibrational spectrum is well described by the calculated spectrum of a C–H···O bonded dimer, which accounts for the symmetry decrease and the intermolecular interactions in the solid. Spectral evidence indicates both C–H···O and O–H···O hydrogen bonds are formed in the MTO/meth-

anol solutions. The Re=O stretching mode is sensitive to hydrogen bonding, but the major effects of intermolecular association are observed in the β C–H and ν C–H modes of MTO. Ab initio calculations for the MTO/methanol system predict the coexistence of both the Lewis adduct and the hydrogen-bonded complex, with an energy difference of ca. 1.2 kJ·mol^{−1}.

(© Wiley-VCH Verlag GmbH & Co. KGaA, 69451 Weinheim, Germany, 2005)

Introduction

Methyltrioxorhenium (MTO) is a small transition metal organometallic molecule that has been recently studied for its properties in catalysis, mainly as an oxidation catalyst,^[1] see Scheme 1.



Scheme 1.

The structure of this compound has been previously reported.^[2–6] These studies include single crystal neutron diffraction structure determination,^[3] as well as several vibrational studies combined with ab initio calculations.^[2,4–6] However, some questions concerning the intermolecular interactions in the liquid and solid phases still remain. In a recent work by Gisdakis et al., it was proposed that MTO can associate into dimers through oxo-bridges,^[6] where two Re atoms are bound by two Re–O–Re bridges in order to preserve the stoichiometry. Ab initio calculations predicted that the formation of the four proposed geometries would

be endothermic, with dimerization energies of between 7.1 kJ·mol^{−1} and 148.4 kJ·mol^{−1}.^[6]

In this work, the role of C–H···O interactions in the structure of MTO is studied by vibrational spectroscopy and combined with ab initio calculations. FT-Raman spectra were obtained for the solid phase and as a function of concentration in different solvents. In addition, ab initio calculations were carried out in order to elucidate the structure and energy of possible C–H···O bonded forms and to simulate the corresponding vibrational spectra.

Results and Discussion

Figure 1 presents the fully optimised structure of MTO (a) and of the lowest energy MTO hydrogen-bonded dimer (b).

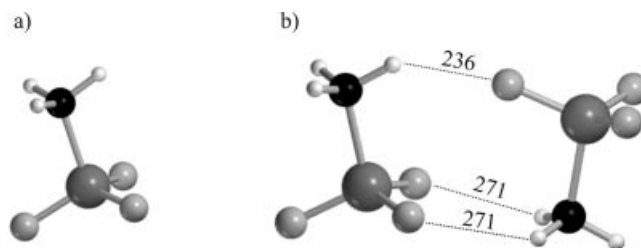


Figure 1. DFT-optimised geometries for a) monomer and b) dimer MTO structures. Distances are in pm.

This MTO dimer – corresponding to a real minimum, i.e. without negative eigenvalues from the frequency calculations – was found to be the most stable configuration among the several MTO dimers tested, and presents three

[a] Departamento de Química, CICECO, Universidade de Aveiro, Campus de Santiago, 3810-193 Aveiro, Portugal
Fax: +351-234-370-084
E-mail: pvaz@dq.ua.pt

[b] Present address: DQB-FCUL, Ed. C8, Campo Grande, 1749-016 Lisboa, Portugal
Fax: +351-217-500-994
E-mail: pmvaz@fc.ul.pt

C–H \cdots O hydrogen bond contacts. The dimerisation energy is $-21.8\text{ kJ}\cdot\text{mol}^{-1}$ (without corrections) and $-15.9\text{ kJ}\cdot\text{mol}^{-1}$ (after CP and ZPVE corrections), falling in the expected range for this type of interaction.^[7–14] These values show that a C–H \cdots O bonded dimer is clearly more stable than the previously reported dimers based on oxygen bridges.^[6] In fact, the dimerisation energy for oxygen bridged dimers, evaluated at the same level of theory, ranges from $7.1\text{ kJ}\cdot\text{mol}^{-1}$ to $148.4\text{ kJ}\cdot\text{mol}^{-1}$ as mentioned above.

The optimised ab initio geometry for the dimer is in very good agreement with the structure determined by neutron diffraction for the solid,^[3] considering the limitations of the “isolated dimer” approach (in the crystal, each molecule has several neighbours), whose structure is represented in Figure 2.

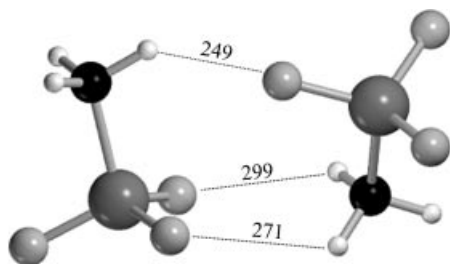


Figure 2. Representation of the interaction motif from the solid structure unit cell of MTO as determined by neutron diffraction.^[3] Distances are in pm.

From the three C–H \cdots O hydrogen bond contacts of the calculated geometry, one is clearly favoured by the geometrical orientation (C–H \cdots O angle: 141°) over the other two (C–H \cdots O angle: 128°), which results in a stronger C–H \cdots O contact. The corresponding H \cdots O contact distance (236 pm – ab initio, 249 pm – neutron diffraction) is clearly shorter than the remaining ones (271 pm – ab initio, 299 pm – neutron diffraction). In addition, the bond length of the C–H donor group of the most favoured contact is shorter than the others (ca. 0.1 pm – ab initio, 1.4 pm neutron diffraction). The shortening of the C–H bond length involved in the strongest C–H \cdots O contact (an effect leading to the increase of the corresponding stretching frequency and to the designation of “blue-shifting hydrogen bond”) indicates that the behaviour of the C(sp³)–H \cdots O=Re interaction is similar to that of C(sp³)–H \cdots O=C.

Figure 3 depicts the comparison between the experimental FT-Raman spectrum and the calculated spectra for both the monomer and the C–H \cdots O bonded dimer. The calculated spectrum for the monomer is clearly oversimplified, as the single molecule model is inadequate to describe the crystal. However, there is an excellent agreement between the calculated and the experimental spectra for the dimer. Although the full description of the solid-state spectra would require a more sophisticated approach, this simple model has the merit of accounting for both the effects of the symmetry reduction and the effects of the most relevant intermolecular contacts. In particular, the magnitude of the splitting of the modes at ca. 750 , 950 , 1400 , and 3000 cm^{-1} is correctly predicted from the fully optimized geometry.

The comparison between the calculated vibrational spectra of the MTO dimer and the experimental vibrational spectra of solid MTO is presented in Table 1 (the full assignment of the vibrational spectra has already been proposed by Parker et al.^[5]). The approximate description of the vibrational modes presented in Table 1 assumes that the CH₃ReO₃ molecule is built from two XY₃ independent fragments. In this way, the 18 normal modes are described as 2×3 vXY stretching modes (3 vCH and 3 vReO), 2×5 XY₃ bending modes ($3\times\beta\text{CH}_3 + 2\times\text{CH}_3$ rocking and $3\times\beta\text{ReO}_3 + 2\times\text{ReO}_3$ rocking), one interfragment stretching mode (vC–Re) and one interfragment torsional mode (described as τCH_3 , since the methyl group is the lighter fragment).

There is an excellent agreement between calculated and experimental assignments, but the results from ab initio calculations with the dimer model suggest a couple of changes relative to the previous vibrational studies.^[2,5] The most obvious difference is related to the bands left unassigned previously by Parker et al.^[5] (e.g. the bands at 2988 , 1364 , and 946 cm^{-1}) and not observed in the partial assignment of Mink et al.^[2] (e.g. the second component of the 2986 – 2990 doublet). These bands are now clearly related with modes of the C–H \cdots O bonded dimer. In some cases, the effect of the C–H \cdots O contact yields a noticeable effect on the vibrational mode. For instance, according to ab initio calculations, C–H \cdots O hydrogen bonds in the dimer produce a C–H bond shortening relative to the monomer, with a corresponding blue shift of the vC–H mode. The effect is also observed for the $\beta\text{C–H}$ and $\gamma\text{C–H}$ modes, which are calculated at 1377 cm^{-1} and 763 cm^{-1} , respectively, blue-shifted from the predicted fundamentals of the monomer. In this way, the highest wavenumber vC–H, $\beta\text{C–H}$ and $\gamma\text{C–H}$ bands have been assigned to the C–H bond engaged in the strongest C–H \cdots O contact.

Another point of interest is the location of the H \cdots O hydrogen bond stretching modes. Ab initio calculations predict the three vH \cdots O modes at 26 , 61 and 76 cm^{-1} , the last one being related to the strongest C–H \cdots O bond. In the low wavenumber region, there are several bands observed in the INS spectrum – already assigned to librational and translational modes^[5] – and a very weak band in the Raman spectrum at 84 cm^{-1} . On the basis of the proximity of the calculated wavenumber value and weak intensity, we tentatively assign the Raman band at 84 cm^{-1} to the strongest vH \cdots O mode (predicted at 76 cm^{-1} from ab initio calculations). It should be stressed, however, that this is not a conclusive assignment and other bands (e.g. INS bands at 101 cm^{-1} or 50 cm^{-1}) can alternatively be related with this mode (Table 1).

In order to evaluate the relevance of C–H \cdots O interactions in MTO/solvent systems, several solutions of MTO in solvents with acceptor/donor (e.g. CH₃OH, CD₃OD) and weak donor/non-acceptor (e.g. CD₂Cl₂) properties were prepared.

Ab initio calculations of MTO/solvent complexes were also performed, in order to evaluate the possible interactions between MTO and the solvents. As expected, the in-

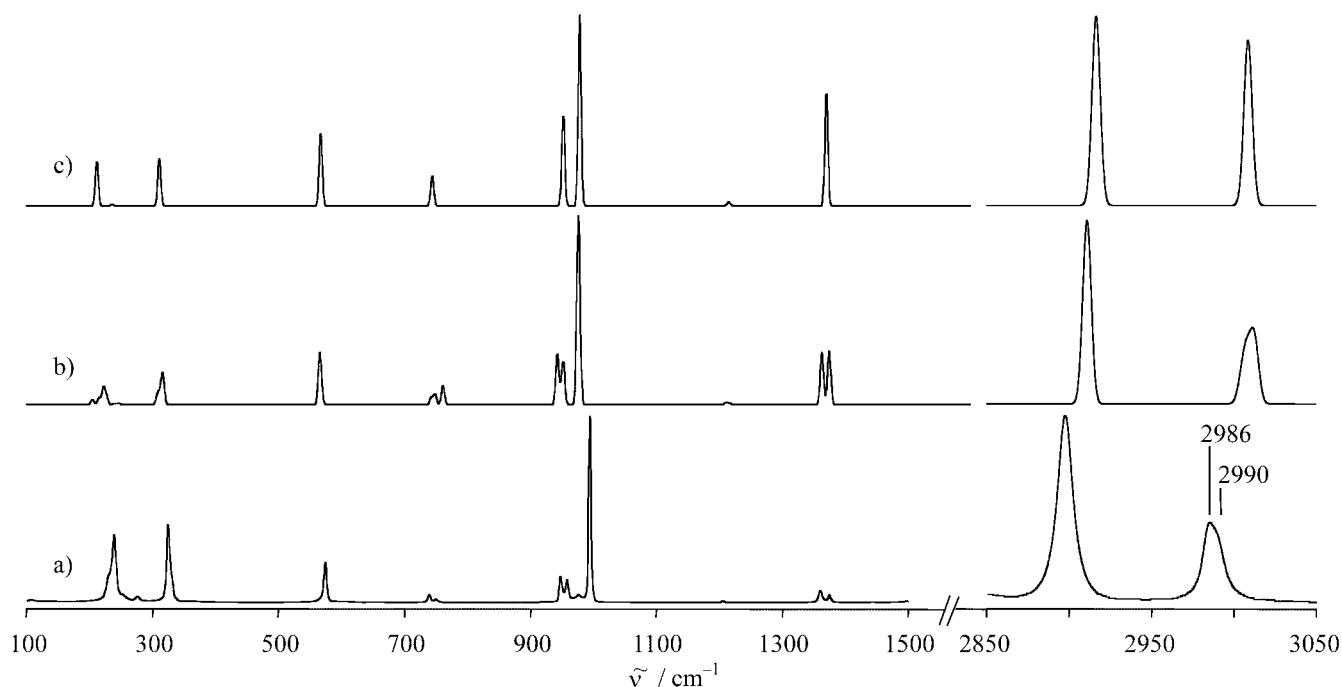


Figure 3. Raman spectra of MTO: a) experimental solid at room temperature, b) ab initio dimer simulation and c) ab initio monomer simulation.

Table 1. Comparison and assignment of the infrared, Raman, INS and ab initio vibrational frequencies ($\tilde{\nu}/\text{cm}^{-1}$) of MTO.

IR	Raman	INS ^[5]	ab initio calc.	Mode	Assignment
2990 (m, sh)	2990 (m, sh)	—	3019	ν_1	$\nu\text{C-H}(\cdots\text{O})$
2986 (m)	2986 (m)	—	3014	ν_2	$\nu\text{C-H asym}$
2898 (m)	2898 (s)	—	2921	ν_3	$\nu\text{C-H sym}$
1373 (w, sh)	1375 (w)	—	1377	ν_4	$\beta\text{C-H}(\cdots\text{O}) \text{ asym}$
1359 (m)	1361 (w)	—	1373	ν_5	$\beta\text{C-H asym}$
1205 (w)	1206 (vw)	—	1217	ν_6	$\beta\text{C-H sym}$
997 (vs)	995 (vs)	—	982	ν_7	$\nu\text{Re=O sym}$
959 (vs)	960 (m)	—	954	ν_8	$\nu\text{Re=O asym}$
948 (vs)	949 (m)	938	944	ν_9	$\nu\text{Re=O asym}$
—	751 (vw)	—	763	ν_{10}	$\gamma\text{C-H}(\cdots\text{O}) \text{ rock}$
739 (m)	740 (w)	738	747	ν_{11}	$\gamma\text{C-H rock}$
571 (m)	575 (s)	573	570	ν_{12}	$\nu\text{Re-C}$
—	331 (w, sh)	—	317	ν_{13}	$\beta\text{Re=O sym}$
322 (m)	325 (vs)	—	313	ν_{14}	$\beta\text{Re=O sym}$
—	276 (w)	—	237	ν_{15}	$\beta\text{Re=O}$
—	240 (vs)	241	228	ν_{16}	$\gamma\text{Re=O rock}$
—	231 (sh)	232	213	ν_{17}	$\gamma\text{Re=O rock}$
—	—	199	184	ν_{18}	τCH_3
—	107 (w)	109	—	—	—
—	84 (vw)	101, 50	76	—	$\nu\text{H}\cdots\text{O}$

teraction of MTO with CD_2Cl_2 is quite feeble and can be neglected. A different situation arises with methanol. Methanol molecules can interact with MTO either as hydrogen-bond donor or hydrogen-bond acceptor. The formation of a MTO/methanol Lewis acid/base adduct has been described previously by Herrmann et al., on the basis of ^{17}O -NMR spectroscopic data.^[15] Figure 4 shows the energy minimized structure for the MTO/methanol hydrogen-bonded complex and for the MTO/methanol Lewis adduct. The hydrogen bonded complex presents a six-membered ring built from $\text{O-H}\cdots\text{O}$ $\text{C-H}\cdots\text{O}$ short contacts. In contrast, the adduct geometry only allows a distorted $\text{C-H}\cdots\text{O}$ contact. A rel-

evant feature of Figure 4 is the small energy difference found between these two forms of MTO/methanol association (ca. $1.2 \text{ kJ}\cdot\text{mol}^{-1}$ after ZPVE correction), which strongly suggests that both forms can coexist in solution.

Figure 5 shows the Raman spectra of the MTO solutions in the Re=O and C-H stretching regions. These vibrational modes are clearly sensitive to the presence of $\text{C-H}\cdots\text{O}$ interactions, as well as stronger $\text{O-H}\cdots\text{O}(\text{=Re})$ hydrogen bonds.

In the $\nu\text{Re=O}$ wavenumber region ($920\text{--}1020 \text{ cm}^{-1}$), several changes in the band profiles can be observed. Dilution in CD_2Cl_2 produces a shift to higher wavenumbers relative to the solid. This shift can be associated with the interac-

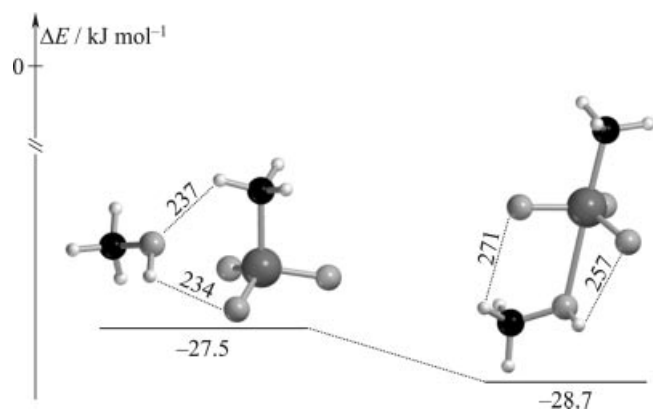


Figure 4. Optimised geometry of the lowest energy MTO/methanol complex based on O–H···O and C–H···O hydrogen bonds, and of the MTO/methanol Lewis adduct. Distances are in pm.

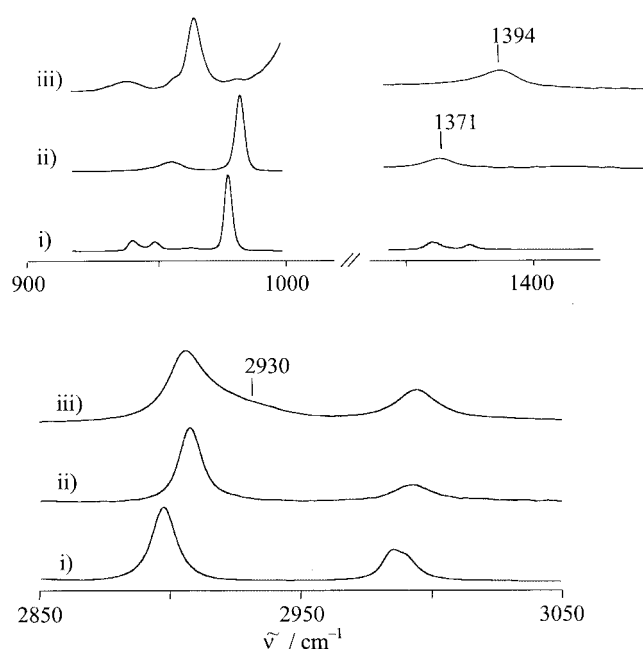


Figure 5. Raman spectra at room temperature of MTO solutions in various solvents in the $\nu\text{Re}=\text{O}$, $\beta\text{C}-\text{H}$ and $\nu\text{C}-\text{H}$ mode regions: i) pure solid, ii) 5% solution in CD_2Cl_2 and iii) 5% solution in CH_3OH or CD_3OD .

tion-free MTO molecules, as CD_2Cl_2 is not expected to interact with MTO, due to low-polarity of the solvent. Another noticeable effect is the merging of the two $\nu\text{Re}=\text{O}$ asymmetric modes into a single broad feature, which is in agreement with the higher symmetry of MTO molecules in solution relative to the solid.

The dilution in methanol yields a large shift towards lower wavenumbers and a marked broadening of the $\nu\text{Re}=\text{O}$ band. This large shift can be ascribed to the formation of Lewis adducts and a hydrogen-bonded complex between methanol and MTO, according to *ab initio* results described above. The presence of four bands in the $\nu\text{Re}=\text{O}$ region of methanol solutions is consistent with the coexist-

ence of the adduct and the hydrogen-bonded complex. In fact, the observed spectrum can be qualitatively described by the sum of the calculated spectra for the two species.

The same general behaviour is observed in the $\beta\text{C}-\text{H}$ wavenumber region ($1350\text{--}1450\text{ cm}^{-1}$). However, the large shift observed from CD_2Cl_2 to methanol solutions can not be explained by bulk solvent effects, such as the change in the dielectric environment,^[16] and is consistent with the presence of more specific interactions. According to the *ab initio* calculations, the MTO methyl group vibrations are virtually insensitive to the formation of the MTO/methanol adduct. On the other hand, C–H···O hydrogen bonds, such as those described in Figure 4, produce wavenumber shifts of the $\beta\text{C}-\text{H}$ modes of ca. 23 cm^{-1} , in agreement with the observed value. These hydrogen bonds are expected to occur even for the MTO molecules already engaged in a MTO/methanol adduct (Figure 6). The MTO methyl group can interact through C–H···O hydrogen bonding with three surrounding methanol molecules, and the presence of such interactions can also explain the large asymmetry of the band.

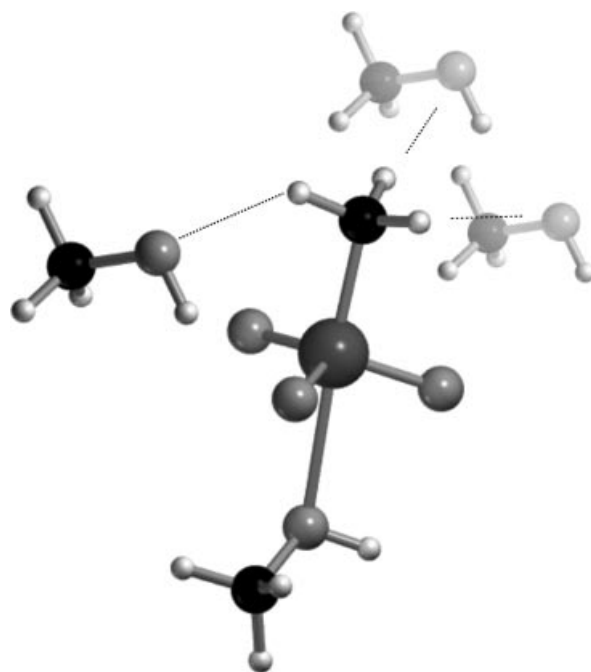


Figure 6. Optimised geometry for the interaction of the MTO/methanol Lewis adduct ($\text{O}\rightarrow\text{Re}$ bond length is 264 pm) with a second methanol molecule which is hydrogen bonded ($\text{H}\cdots\text{O}$ distance is 245 pm). The shadowed methanol molecules represent additional C–H···O contacts assumed to occur in the solution.

In the $\nu\text{C}-\text{H}$ wavenumber region ($2850\text{--}3050\text{ cm}^{-1}$) some changes are also observed. The dilution in methanol gives rise to a general blue shift of all the $\nu\text{C}-\text{H}$ bands. This effect is expected from the bulk solvent effects, due to the change of the dielectric constant.^[16] In addition, there is an intensity increase in the higher wavenumber side of the band at 2906 cm^{-1} , leading to a clear band asymmetry. The effect is seen on the symmetric mode and not in the asymmetric ones, which is unexpected for a symmetry-breaking interac-

tion. Possible explanations are (i) the weakness of the effect (can be hidden due to band broadness) and (ii) the averaging effect of multiple interactions. By comparison with the β C–H region, this band asymmetry can be ascribed to the multiple C–H \cdots O interactions between MTO and methanol solvent molecules. As stated before, C–H \cdots O hydrogen bonds are predicted to result in the blue-shift of the corresponding ν C–H modes. Being so, the intensity increase in the 2930 cm^{-1} region may be ascribed to blue-shifting C–H \cdots O hydrogen bonds.

Conclusions

The present work presents evidence of intermolecular interactions through C–H \cdots O hydrogen bonds in solid MTO. The shortening of the C–H bond length involved in the strongest C–H \cdots O hydrogen bond (leading to the blue-shift of the corresponding C–H stretching frequency by ca. 23 cm^{-1}) indicates that the behaviour of the C(sp³)–H \cdots O=Re interaction is similar to that of C(sp³)–H \cdots O=C. To the best of our knowledge, this is the first report of a blue-shifting C–H \cdots O hydrogen bond involving a Re=O acceptor group. Dilution of MTO in the non-polar solvent CD₂Cl₂ yields vibrational features easily interpreted in terms of isolated MTO molecules. On the other hand, with dilution in methanol, the spectral changes are complex and not easily interpreted. The presence of a MTO/methanol Lewis adduct, already described, can account for some of the changes. Nevertheless, a few other changes, such as those observed in the C–H bending and stretching modes of MTO, fit the changes expected from C–H \cdots O hydrogen bonds. The presence of such interactions is also supported by ab initio calculations, which predict a comparable stability for the MTO/methanol Lewis adduct and for the MTO/methanol hydrogen-bonded complex.

Experimental Section

General Remarks: All reagents and solvents were provided by Aldrich Co. and used as received. Raman spectra were recorded on a Jobin–Yvon T64000 spectrometer with a CCD detector, using the 514.5 nm line of an Ar⁺ laser (Coherent-Inova 90) and on a FT Bruker RFS-100 spectrometer using a Nd:YAG laser (Coherent Compass-1064/500N) with excitation wavelength of 1064 nm, using 2 cm^{-1} resolution. The liquid samples were sealed in Kimax glass capillaries (i.d. 0.8 mm).

Ab initio calculations were performed using the Gaussian 98W program package, rev. A.11.^[17] Molecular structures were fully optimised without constraints at the B3LYP with ECP's on the Re atom (short core approximation) and 6-311G(d,p) on all the remaining atoms. The basis set superposition error (BSSE) correction for the dimerisation energies has been estimated by counterpoise

calculations using the MASSAGE option of Gaussian 98W. Harmonic vibrational wavenumbers were calculated at the level of theory and scaled by an adequate factor in order to provide the best fit with experimental results.

Acknowledgments

The authors thank the Portuguese Foundation for Science and Technology, FCT, for the financial support (research project POCTI/QUI/35408/99, co-financed by the European Community Fund FEDER). PV thanks FCT for a Ph.D. research grant.

- [1] C. C. Romão, F. E. Kühn, W. A. Herrmann, *Chem. Rev.* **1997**, *97*, 3197–3246.
- [2] J. Mink, G. Keresztury, A. Stirling, W. A. Herrmann, *Spectrochim. Acta A* **1994**, *50*, 2039–2057.
- [3] W. A. Herrmann, W. Scherer, R. W. Fischer, J. Blümel, M. Kleine, W. Mertin, R. Gruehn, J. Mink, H. Boysen, C. C. Wilson, R. M. Ibberson, L. Bachmann, M. Mattner, *J. Am. Chem. Soc.* **1995**, *117*, 3231–3243.
- [4] S. Köstlmeier, G. Pacchioni, W. A. Herrmann, N. Rösch, *J. Organomet. Chem.* **1996**, *514*, 111–117.
- [5] S. F. Parker, H. Herman, *Spectrochim. Acta A* **2000**, *56*, 1123–1129.
- [6] P. Gisdakis, N. Rösch, É. Bencze, J. Mink, I. S. Gonçalves, F. E. Kühn, *Eur. J. Inorg. Chem.* **2001**, 981–991.
- [7] X. Li, L. Liu, H. B. Schlegel, *J. Am. Chem. Soc.* **2002**, *124*, 9639–9647.
- [8] N. Karger, A. M. Amorim da Costa, P. J. A. Ribeiro-Claro, *J. Phys. Chem. A* **1999**, *103*, 8672–8677.
- [9] M. P. M. Marques, A. M. Amorim da Costa, P. J. A. Ribeiro-Claro, *J. Phys. Chem. A* **2001**, *105*, 5292–5297.
- [10] P. J. A. Ribeiro-Claro, M. P. M. Marques, A. M. Amado, *ChemPhysChem* **2002**, *3*, 599–606.
- [11] P. J. A. Ribeiro-Claro, M. G. B. Drew, V. Felix, *Chem. Phys. Lett.* **2002**, *356*, 318–324.
- [12] P. D. Vaz, P. J. A. Ribeiro-Claro, *J. Phys. Chem. A* **2003**, *107*, 6301–6305.
- [13] A. Goel, C. N. R. Rao, *J. Chem. Soc. Faraday Trans.* **1971**, 2828–2834.
- [14] V. I. Bruskov, V. N. Bushuev, M. S. Okon, N. V. Shulyupina, V. I. Poltev, *Biopolymers* **1989**, *28*, 589–604.
- [15] W. A. Herrmann, F. E. Kühn, P. W. Roesky, *J. Organomet. Chem.* **1995**, *485*, 243–251.
- [16] P. J. A. Ribeiro-Claro, P. D. Vaz, *Chem. Phys. Lett.* **2004**, *390*, 358–361.
- [17] M. J. Frisch, G. W. Trucks, H. B. Schlegel, G. E. Scuseria, M. A. Robb, J. R. Cheeseman, V. G. Zakrzewski, J. A. Montgomery Jr., R. E. Stratmann, J. C. Burant, S. Dapprich, J. M. Millam, A. D. Daniels, K. N. Kudin, M. C. Strain, O. Farkas, J. Tomasi, V. Barone, M. Cossi, R. Cammi, B. Mennucci, C. Pomelli, C. Adamo, S. Clifford, J. Chterski, G. A. Petersson, P. Y. Ayala, Q. Cui, K. Morokuma, D. K. Malick, A. D. Rabuck, K. Raghavachari, J. B. Foresman, J. Cioslowski, J. V. Ortiz, A. G. Baboul, B. B. Stefanov, G. Liu, A. Liashenko, P. Piskorz, I. Komaromi, R. Gomperts, R. L. Martin, D. J. Fox, T. Keith, M. A. Al-Laham, C. Y. Peng, A. Nanayakkara, C. Gonzalez, M. Challacombe, P. M. W. Gill, B. Johnson, W. Chen, M. W. Wong, J. L. Andres, C. Gonzalez, M. Head-Gordon, E. S. Replogle, J. A. Pople, *Gaussian 98, Revision A.11*, Gaussian, Inc., Pittsburgh, PA, **1998**.

Received: September 28, 2004